Recent developments in the CTEQ-TEA global analysis: CT18CS and CT18As

Tie-Jiun Hou
（侯铁君）
University of South China

January 10th, 2023 at USTC

CTEQ

Global PDF Analysis with Lattice Input

CT18As

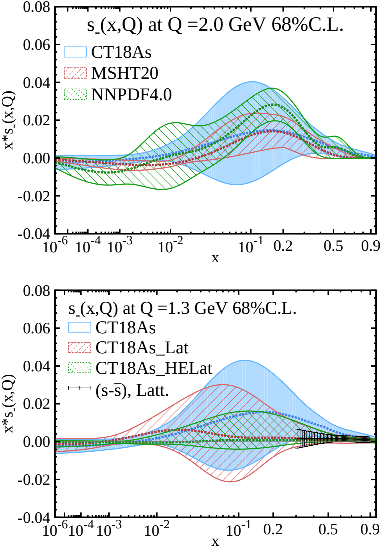

arXiv:2211.11064

CT18CS

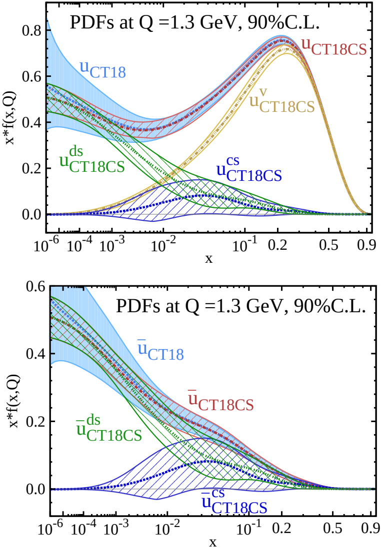

PRD106(2022)9,096008

CT18 in a nutshell

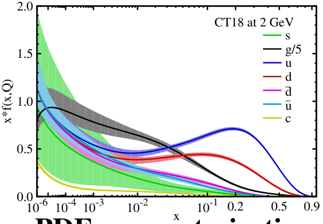

- Start from **CT14-HERAII**:
  (PRD95,034003(2017), T.-J. Hou *et al*)
  HERAII combined data released after publication of CT14
  (PRD93,033006(2016), S. Dulat *et al*).
- Examine a **wide range of non-perturbative PDF parameterizations**.
- Use as much relevant **LHC Run II data** as possible; using applgrid/fastNLO interfaces to data sets, with NNLO/NLO K-factors, or fastNNLO tables in the case of top pair (single and double differential) data.
- Implement a **parallelization** of the global PDF fitting to allow for faster turn-around time.
- Use diverse statistical techniques (**PDFSense**, **ePump**, **Gaussian variables**, **Lagrange Multiplier** scans) to examine agreement between experiments.

Data sets included in CT18 - old data

ID#	Experimental data set		$N_{pt,E}$	χ^2_E	$\chi^2_E/N_{pt,E}$	S_E
160	HERAI+II 1 fb^{-1}, H1 and ZEUS NC and CC $e^{\pm}p$ reduced cross sec. comb.	[29]	1120	1408(1378)	1.3(1.2)	5.7(5.1)
101	BCDMS F_2^p	[62]	337	374 (384)	1.1(1.1)	1.4(1.8)
102	BCDMS F_2^d	[63]	250	280 (287)	1.1(1.1)	1.3(1.6)
104	NMC F_2^d/F_2^p	[64]	123	126 (116)	1.0(0.9)	0.2(-0.4)
108†	CDHSW F_2^p	[65]	85	85.6 (86.8)	1.0(1.0)	0.1(0.2)
109†	CDHSW $x_B F_3^p$	[65]	96	86.5 (85.6)	0.9(0.9)	-0.7(-0.7)
110	CCFR F_2^p	[66]	69	78.8(76.0)	1.1(1.1)	0.9(0.6)
111	CCFR $x_B F_3^p$	[67]	86	33.8(31.4)	0.4(0.4)	-5.2(-5.6)
124	NuTeV $\nu\mu\mu$ SIDIS	[68]	38	18.5(30.3)	0.5(0.8)	-2.7(-0.9)
125	NuTeV $\bar{\nu}\mu\mu$ SIDIS	[68]	33	38.5(56.7)	1.2(1.7)	0.7(2.5)
126	CCFR $\nu\mu\mu$ SIDIS	[69]	40	29.9(35.0)	0.7(0.9)	-1.1(-0.5)
127	CCFR $\bar{\nu}\mu\mu$ SIDIS	[69]	38	19.8(18.7)	0.5(0.5)	-2.5(-2.7)
145	H1 σ_r^b	[70]	10	6.8(7.0)	0.7(0.7)	-0.6(-0.6)
147	Combined HERA charm production	[71]	47	58.3(56.4)	1.2(1.2)	1.1(1.0)
169	H1 F_L	[32]	9	17.0(15.4)	1.9(1.7)	1.7(1.4)
201	E605 Drell-Yan process	[72]	119	103.4(102.4)	0.9(0.9)	-1.0(-1.1)
203	E866 Drell-Yan process $\sigma_{pd}/(2\sigma_{pp})$	[73]	15	16.1(17.9)	1.1(1.2)	0.3(0.6)
204	E866 Drell-Yan process $Q^3 d^2\sigma_{pp}/(dQdx_F)$	[74]	184	244 (240)	1.3(1.3)	2.9(2.7)
225	CDF Run-1 lepton A_{ch}, $p_{T\ell} > 25$ GeV	[75]	11	9.0(9.3)	0.8(0.8)	-0.3(-0.2)
227	CDF Run-2 electron A_{ch}, $p_{T\ell} > 25$ GeV	[76]	11	13.5(13.4)	1.2(1.2)	0.6(0.6)
234	DØ Run-2 muon A_{ch}, $p_{T\ell} > 20$ GeV	[77]	9	9.1(9.0)	1.0(1.0)	0.2(0.1)
260	DØ Run-2 Z rapidity	[78]	28	16.9(18.7)	0.6(0.7)	-1.7(-1.3)
261	CDF Run-2 Z rapidity	[79]	29	48.7(61.1)	1.7(2.1)	2.2(3.3)
266	CMS 7 TeV 4.7 fb^{-1}, muon A_{ch}, $p_{T\ell} > 35$ GeV	[80]	11	7.9(12.2)	0.7(1.1)	-0.6(0.4)
267	CMS 7 TeV 840 pb^{-1}, electron A_{ch}, $p_{T\ell} > 35$ GeV	[81]	11	4.6(5.5)	0.4(0.5)	-1.6(-1.3)
268‡‡	ATLAS 7 TeV 35 pb^{-1} W/Z cross sec., A_{ch}	[82]	41	44.4 (50.6)	1.1(1.2)	0.4(1.1)
281	DØ Run-2 9.7 fb^{-1} electron A_{ch}, $p_{T\ell} > 25$ GeV	[83]	13	22.8(20.5)	1.8(1.6)	1.7(1.4)
504	CDF Run-2 inclusive jet production	[84]	72	122 (117)	1.7(1.6)	3.5(3.2)
514	DØ Run-2 inclusive jet production	[85]	110	113.8 (115.2)	1.0(1.0)	0.3(0.4)

1xx DIS
2xx Drell-Yan
5xx Jet

- HERA I+II data plays an important role.
- Old fixed target data still have strong impact on PDFs.

LHC data sets included in CT18 - new data

245	1505.07024	LHCb Z (W) muon rapidity at 7 TeV
246	1503.00963	LHCb 8 TeV Z rapidity
249	1603.01803	CMS W lepton asymmetry at 8 TeV
250	1511.08039	LHCb Z (W) muon rapidity at 8 TeV
253	1512.02192	ATLAS 7 TeV Z p_T
542	1406.0324	CMS incl. jet at 7 TeV with R=0.7
544	1410.8857	ATLAS incl. jet at 7 TeV with R=0.6
545	1609.05331	CMS incl. jet at 8 TeV with R=0.7
573	1703.01630	CMS 8 TeV $t\bar{t}$ (p_T, y_t) double diff. distributions
580	1511.04716	ATLAS 8 TeV $t\bar{t}$ p_T and $m_{t\bar{t}}$ diff. distributions
248	1612.03016	ATLAS 7 TeV Z and W rapidity $\rightarrow$ CT18A PDFs

(PRD, arXiv: 1912.10053, T.- J. Hou *et al.*)

Theory calculations @NNLO

Obs.	Expt.	fast table	NLO code	K-factors	R,F scales
Inclusive jet	ATL 7 CMS 7/8	APPLgrid fastNLO	NLOJet++	NNLOJet	p_T, p_T^1
p_T^Z	ATL 8	APPLgrid	MCFM	NNLOJet	$\sqrt{Q^2 + p_{T,Z}^2}$
W/Z rapidity W asymmetry	LHCb 7/8 ATL 7 CMS 8	APPLgrid	MCFM/aMCfast	FEWZ/MCFM	$M_{W,Z}$
DY (low,high mass)	ATL 7/8 CMS 8	APPLgrid	MCFM/aMCfast	FEWZ/MCFM	Q_{ll}
$t\bar{t}$	ATL 8 CMS 8	fastNNLO			$\frac{H_T}{4}, \frac{m_T}{2}$

- For Drell-Yan data and jet data, NNLO prediction are down by using NLO prediction from applgrid/fastNLO times NNLO/NLO K-factor.
- For $t\bar{t}$ data, NNLO prediction are down by using NNLO prediction from fastNLO directly.

  the MC integration of NNLO cross sections.

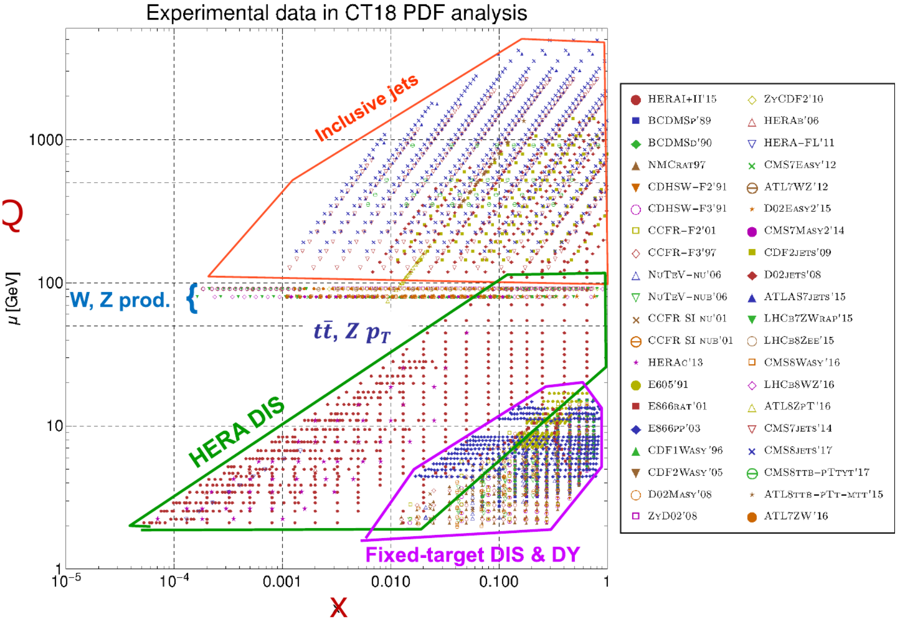

Experimental data in CT18 PDF analysis
Inclusive jets
W, Z prod.
$t\bar{t}$, Z p_T
HERA DIS
Fixed-target DIS & DY
Q
μ [GeV]
x
1000
100
10
1
10^{-5}
10^{-4}
0.001
0.010
0.100
1
HERAI+II'15
BCDMSp'89
BCDMSd'90
NMCrat97
CDHSW-F2'91
CDHSW-F3'91
CCFR-F2'01
CCFR-F3'97
NuTeV-nu'06
NuTeV-nub'06
CCFR SI nu'01
CCFR SI nub'01
HERAc'13
E605'91
E866rat'01
E866pp'03
CDF1Wasy'96
CDF2Wasy'05
D02Masy'08
ZyD02'08
ZyCDF2'10
HERAb'06
HERA-FL'11
CMS7Easy'12
ATL7WZ'12
D02Easy2'15
CMS7Masy2'14
CDF2jets'09
D02jets'08
ATLAS7jets'15
LHCb7ZWrap'15
LHCb8Zee'15
CMS8Wasy'16
LHCb8WZ'16
ATL8ZpT'16
CMS7jets'14
CMS8jets'17
CMS8ttb-pTtyt'17
ATL8ttb-pTt-mtt'15
ATL7ZW'16

Non-perturbative forms of PDFs in CT18 at $Q_0 = 1.3$GeV

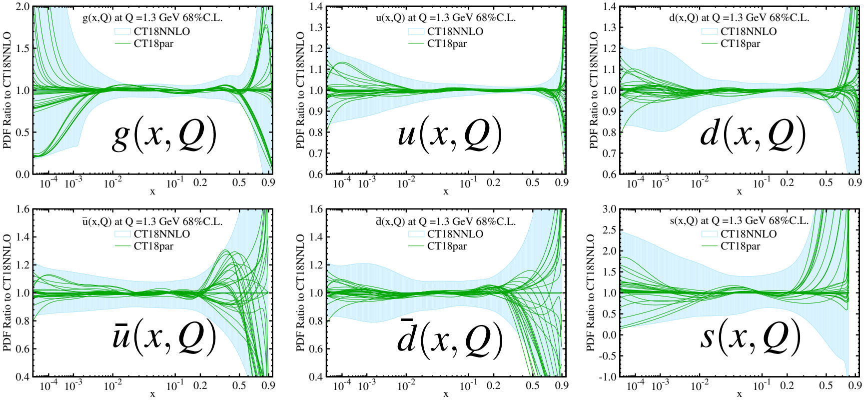

- CT18 – sample result of exploring various non-perturbative parametrization forms at $Q_0 = 1.3$ GeV.
- There is no data to constrain very large and very small x region.

Non-perturbative forms of PDFs in CT18 at $Q_0 = 1.3$ GeV

In CT18, 6 d.o.f of partons are parametrized at $Q_0 = m_c = 1.3$ GeV $\gg \Lambda_{QCD}$,

$$g, \quad u^v, \quad d^v, \quad \bar{u}, \quad \bar{d}, \quad s.$$

Where $\bar{s}(x) \equiv s(x)$ is assumed, and $u = u^v + \bar{u}$ and $d = d^v + \bar{d}$. Heavier parton, like c, b and t, are generated through PDF evolution. The functional form for the 6 parton flavors is

$$f^i(x, Q = Q_0) = a_0^i x^{a_1^i - 1}(1-x)^{a_2^i} P^i(x)$$

- $x \to 0$: $f^i \propto x^{a_1^i - 1}$, Regge-like behavior
- $x \to 1$: $f^i \propto (1-x)^{a_2^i}$, quark counting rules
- $P^i(x; a_3, a_4, \ldots)$: affects intermediate x. In CT18, Bernstein polynomial is applied.

Requirements for PDF parametrization

- Valence quark number sum rule

$$\int_0^1 [u(x) - \bar{u}(x)]dx = 2, \quad \int_0^1 [d(x) - \bar{d}(x)]dx = 1$$

$$\int_0^1 [s(x) - \bar{s}(x)]dx = 0$$

- Momentum sum rule

$$\sum_{a=q,\bar{q},g} \int_0^1 x f_{a/p}(x,Q)dx = 1$$

In total, there are 29 shape parameters used in CT18.
As a result, the full CT18 global fit yields $\chi^2 = 4292$, with a total of 3681 data points, and $\chi^2/N_{pt} = 1.17$.

PDF Luminosities at 13 TeV LHC
CT18, MMHT14 and NNPDF3.1

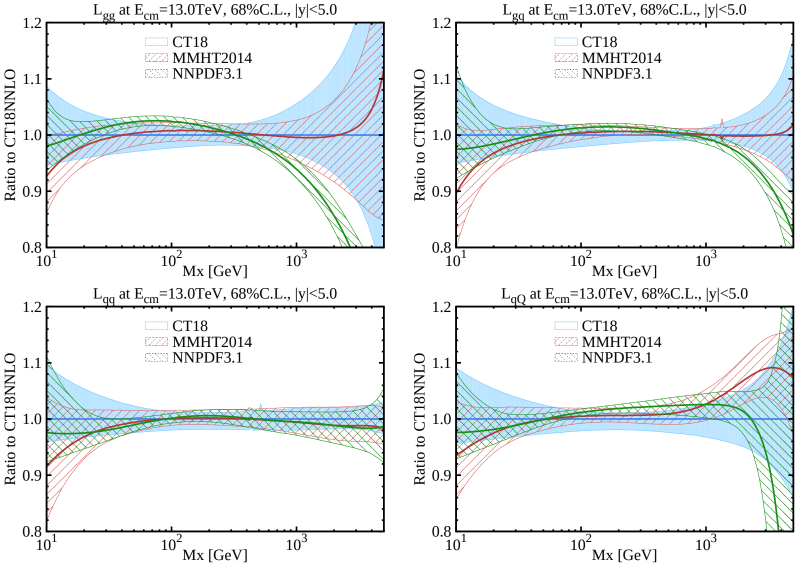

Connected and Disconnected Sea Partons from the CT18 Parametrization of PDFs

In Collaborate with Jian Liang, Keh-Fei Liu,
Mengshi Yan, and C.–P. Yuan

Phys.Rev.D 106 (2022) 9, 096008

Gottfried sum rule

Gottfried sum rule (1967) was originally obtain by assuming $\bar{u}$ and $\bar{d}$ to be the same, which leads to

$$S_G = \int_0^1 \frac{dx}{x}\left[F_2^p(x) - F_2^n(x)\right] = \frac{1}{3}, \quad \text{with } \bar{d}(x) \equiv \bar{u}(x)$$

New Muon Collaboration (NMC PRL 66, 2712 (1991), PRD 50, R1 (1994)), $\mu + p(n) \to \mu + X$, obtained

$$S_G = 0.235 \pm 0.026 \quad (\, Q = 2\,\text{GeV}\,)$$

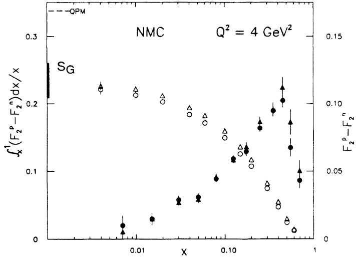

Gottfried sum rule

The alternative expression of Gottfried sum rule is,

$$S_G = \frac{1}{3} - \frac{2}{3}\int_0^1 dx\left(\bar{d}(x) - \bar{u}(x)\right) + O(\alpha_s^2).$$

Hence, NMC data gives

$$\int_0^1 dx\left(\bar{d}(x) - \bar{u}(x)\right) = 0.147 \pm 0.039, \quad \text{at } Q = 2\text{ GeV}$$

The following experiments like HERMES (PLB387, 419 (1996)) and E866 (PRD64, 052002 (2001)) also shown preference of $\bar{u}/\bar{d}$ flavor asymmetry.

Experiment	$\langle Q^2 \rangle$ (GeV^2)	$\int_0^1 [\bar{d}(x) - \bar{u}(x)]dx$
NMC/DIS	4.0	0.147 ± 0.039
HERMES/SIDIS	2.3	0.16 ± 0.03
FNAL E866/DY	54.0	0.118 ± 0.012

What is the origin of $\int dx \left(\bar{d}(x) - \bar{u}(x)\right) \neq 0$?

Hadronic tensor in Euclidean path-integral formalism

Motivated by Hadronic tensor in QCD path-integral formalism in Euclidian space.

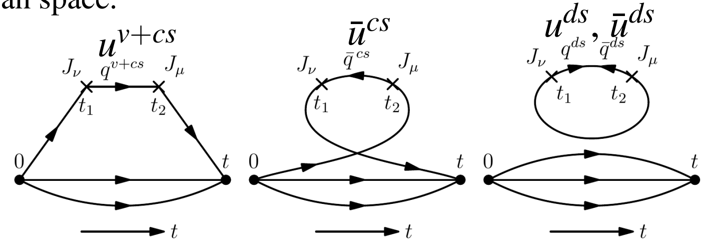

Connected sea(CS) Disconnected sea(DS)

$$\begin{aligned} u &= u^{v+cs} + u^{ds}, \quad & d &= d^{v+cs} + d^{ds} \\ \bar{u} &= \bar{u}^{cs} + \bar{u}^{ds}, \quad & \bar{d} &= \bar{d}^{cs} + \bar{d}^{ds} \end{aligned}$$

Define $u^v \equiv u^{v+cs} - \bar{u}^{cs}$, which is equivalent to defining $u^{cs} \equiv \bar{u}^{cs}$.

$$\begin{aligned} u - \bar{u} &\equiv (u^{v+cs} + u^{ds}) - (\bar{u}^{cs} + \bar{u}^{ds}) = u^v + (u^{ds} - \bar{u}^{ds}) \\ &\neq u^v, \quad \text{unless } u^{ds} = \bar{u}^{ds} \end{aligned}$$

Similarly, $d^v \equiv d^{v+cs} - \bar{d}^{cs}$.

Hadronic tensor in Euclidean path-integral formalism versus Quasi-PDF from Lattice QCD

- Path-Integral Formalism

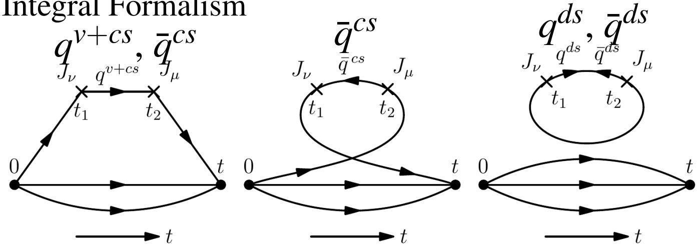

- Quasi-PDF from Lattice QCD

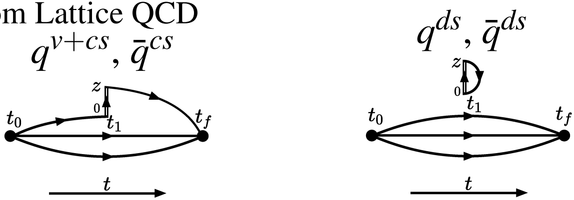

Connected Insertion(CI) Disconnected Insertion(DI)

Quasi PDF results from LP3 and ETMC connected insertion calculation

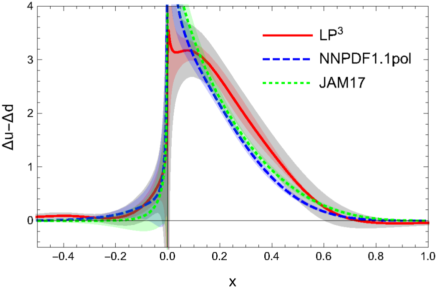

LP3 – H.W. Lin *et al*, PRL, arXiv:1807.07431

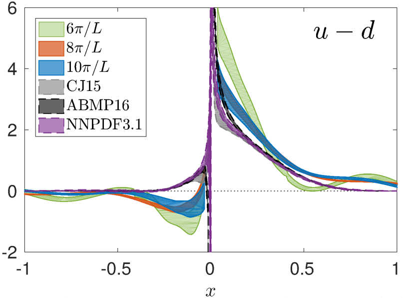

C. Alexandrou *et al*, PRL, arXiv:1803.02685

Where

$$q(x>0) = q^{v+cs}(x), \qquad q(x<0) = -\bar{q}^{cs}$$

Parton degrees of freedom are the same as in hadronic tensor

K.F. Liu, PRD, arXiv:2007.15075

Lattice input to global fitting of PDFs

Lattice result from overlap on $N_f = 2+1$ DWF on 4 lattices, with one at physical pion mass (J. Liang *et al*, χQCD, PRD, arXiv:1901.07526)

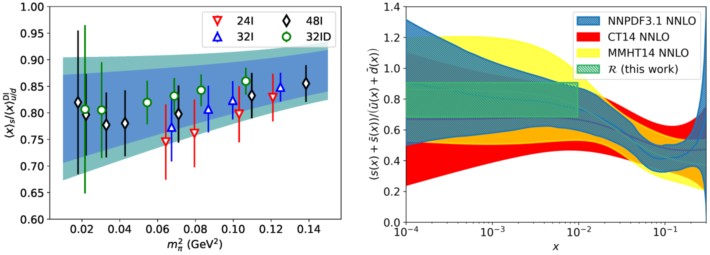

$$\frac{1}{R} = \frac{\langle x\rangle_{s+\bar{s}}}{\langle x\rangle_{\bar{u}+\bar{d}}(DI)}(\text{at } 1.3 \text{ GeV}) = 0.822(69)(78)$$

This is the only Lattice data used in the CT18CS analysis.

Strategy for global analysis in CT18CS

In CT18CS, the non-perturbative PDFs parametrized at $Q_0 = 1.3$ GeV are :

$$g, \quad u^v, \quad d^v, \quad \bar{u}^{cs}, \quad \bar{d}^{cs}, \quad s^{ds}.$$

In this analysis,

- Disconnected Sea (DS) components:
  - Similar to CT18 fit, we assume $\bar{s}(x) = s(x)$. Hence, $s^{ds}(x) = \bar{s}^{ds}(x)$.
  - Likewise, we also assume $u^{ds}(x) = \bar{u}^{ds}(x)$ and $d^{ds}(x) = \bar{d}^{ds}(x)$ for simplicity.
  - Assuming isospin symmetry for $\bar{u}$ and $\bar{d}$ quark PDF

  This leads to

$$u^{ds} = \bar{u}^{ds} = d^{ds} = \bar{d}^{ds} = Rs = R\bar{s},$$

With $1/R = 0.822$ at $Q_0 = 1.3$ GeV.

Parton degrees of freedom at $Q_0 = 1.3$ GeV

- Connected Sea (CS) components:
  We define $u^{cs} \equiv \bar{u}^{cs}$ and $d^{cs} \equiv \bar{d}^{cs}$. They will be separately determined by the global fit, though with the same a_1 and a_2 components.

The physical parton degrees of freedom used in CT18CS are then:

In CT18

$$
\begin{aligned}
g &= g_{par} \\
u^v &= u^v_{par} \\
d^v &= d^v_{par} \\
\bar{u} &= \bar{u}^{cs} + \bar{u}^{ds} = \bar{u}_{par} + Rs_{par} \\
\bar{d} &= \bar{d}^{cs} + \bar{d}^{ds} = \bar{d}_{par} + Rs_{par} \\
s &= \bar{s} = s_{par}
\end{aligned}
$$

In CT18CS

Both CT18 and CT18CS have 6 independent non-perturbative PDF functions, hence 6 parton degrees of freedom, at Q_0 scale.
The PDFs $f(x,Q)$ at $Q > Q_0$ are obtained by applying DGLAP evolution equations, as in CT18.

Global Analysis - CT18

The global analysis of CT18 has already included the data of NMC and E866, and thus reflect the $\bar{u} \neq \bar{d}$.

ID#	Experimental data set		N_{pt}	χ^2	χ^2/N_{pt}	S_E
160	HERAI+II 1 fb^{-1}, H1 and ZEUS NC and CC $e^{\pm}p$ reduced cross sec. comb.	[27]	1120	1408(1378)	1.3(1.2)	5.7(5.1)
101	BCDMS F_2^p	[65]	337	374 (384)	1.1(1.1)	1.4(1.8)
102	BCDMS F_2^d	[66]	250	280 (287)	1.1(1.1)	1.3(1.6)
104	NMC F_2^d/F_2^p ← NMC	[67]	123	126 (116)	1.0(0.9)	0.2(-0.4)
108†	CDHSW F_2^p	[68]	85	85.6 (86.8)	1.0(1.0)	0.1(0.2)
109†	CDHSW F_3^p	[68]	96	86.5 (85.6)	0.9(0.9)	-0.7(-0.7)
110	CCFR F_2^p	[69]	69	78.8(76.0)	1.1(1.1)	0.9(0.6)
111	CCFR xF_3^p	[70]	86	33.8(31.4)	0.4(0.4)	-5.2(-5.6)
124	NuTeV $\nu\mu\mu$ SIDIS	[71]	38	18.5(30.3)	0.5(0.8)	-2.7(-0.9)
125	NuTeV $\bar{\nu}\mu\mu$ SIDIS	[71]	33	38.5(56.7)	1.2(1.7)	0.7(2.5)
126	CCFR $\nu\mu\mu$ SIDIS	[72]	40	29.9(35.0)	0.7(0.9)	-1.1(-0.5)
127	CCFR $\bar{\nu}\mu\mu$ SIDIS	[72]	38	19.8(18.7)	0.5(0.5)	-2.5(-2.7)
145	H1 σ_r^b	[73]	10	6.8(7.0)	0.7(0.7)	-0.6(-0.6)
147	Combined HERA charm production	[74]	47	58.3(56.4)	1.2(1.2)	1.1(1.0)
169	H1 F_L	[30]	9	17.0(15.4)	1.9(1.7)	1.7(1.4)
201	E605 Drell-Yan process	[75]	119	103.4(102.4)	0.9(0.9)	-1.0(-1.1)
203	E866 Drell-Yan process $\sigma_{pd}/(2\sigma_{pp})$ ← E866	[76]	15	16.1(17.9)	1.1(1.2)	0.3(0.6)
204	E866 Drell-Yan process $Q^3 d^2\sigma_{pp}/(dQdx_F)$	[77]	184	244 (240)	1.3(1.3)	2.9(2.7)
225	CDF Run-1 electron A_{ch}, $p_{T\ell} > 25$ GeV	[78]	11	9.0(9.3)	0.8(0.8)	-0.3(-0.2)
227	CDF Run-2 electron A_{ch}, $p_{T\ell} > 25$ GeV	[79]	11	13.5(13.4)	1.2(1.2)	0.6(0.6)
234	DØ Run-2 muon A_{ch}, $p_{T\ell} > 20$ GeV	[80]	9	9.1(9.0)	1.0(1.0)	0.2(0.1)
260	DØ Run-2 Z rapidity	[81]	28	16.9(18.7)	0.6(0.7)	-1.7(-1.3)
261	CDF Run-2 Z rapidity	[82]	29	48.7(61.1)	1.7(2.1)	2.2(3.3)
266	CMS 7 TeV 4.7 fb^{-1}, muon A_{ch}, $p_{T\ell} > 35$ GeV	[83]	11	7.9(12.2)	0.7(1.1)	-0.6(0.4)
267	CMS 7 TeV 840 pb^{-1}, electron A_{ch}, $p_{T\ell} > 35$ GeV	[84]	11	11.8(16.1)	1.1(1.5)	0.3(1.1)
268‡‡	ATLAS 7 TeV 35 pb^{-1} W/Z cross sec., A_{ch}	[85]	41	44.4 (50.6)	1.1(1.2)	0.4(1.1)
281	DØ Run-2 9.7 fb^{-1} electron A_{ch}, $p_{T\ell} > 25$ GeV	[86]	13	22.8(20.5)	1.8(1.6)	1.7(1.4)
504	CDF Run-2 inclusive jet production	[87]	72	122 (117)	1.7(1.6)	3.5(3.2)
514	DØ Run-2 inclusive jet production	[88]	110	113.8 (115.2)	1.0(1.0)	0.3(0.4)

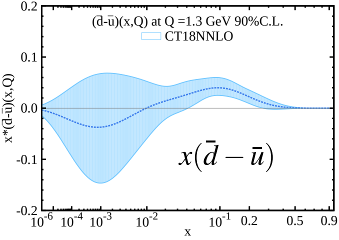

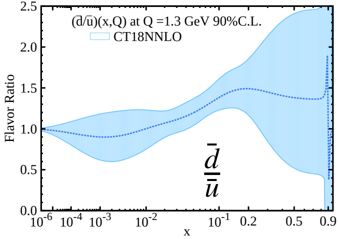

Small-x behavior of CT18CS PDFs

The non-perturbative PDF functions are chosen so that

1. $\bar{d}/\bar{u} \xrightarrow{x\to 0} 1.$ $\Leftarrow$ Isospin symmetry, similar to CT18
2. $\bar{u}^{ds}, \bar{d}^{ds}, \bar{s}^{ds} \xrightarrow{x\to 0} x^{-1}.$ $\Leftarrow$ Similar to CT18
3. $\bar{u}^{cs}, \bar{d}^{cs} \xrightarrow{x\to 0} u^v, d^v.$ $\Leftarrow$ $\bar{q}^{cs}$ is in the connected insertion
4. $d/u \xrightarrow{x\to 1} d/u$ of CT18. $\Leftarrow$ Valence behavior, similar to CT18.
5. $\bar{d}/\bar{u} \xrightarrow{x\to 1} \bar{d}/\bar{u}$ of CT18. $\Leftarrow$ Describe E866 and E906 data.

Where $f^i(x, Q = Q_0) = a_0^i x^{a_1^i - 1}(1-x)^{a_2^i} P^i(x)$

CT18	u^v	d^v	g	$\bar{u}$	$\bar{d}$	s
a_1	0.763	0.763	0.531	−0.022	−0.022	−0.022
a_2	3.036	3.036	3.148	7.737	7.737	10.31
CT18CS	u^v	d^v	g	$\bar{u}^{cs}$	$\bar{d}^{cs}$	s^{ds}
a_1	$0.739^{(3)}$	$0.739^{(3)}$	0.553	$0.739^{(3)}$	$0.739^{(3)}$	$0.000^{(2)}$
a_2	$3.036^{(4)}$	$3.036^{(4)}$	3.371	$7.737^{(5)}$	$7.737^{(5)}$	11.57

CT18CS PDFs

With the input of $\bar{u}^{ds} = \bar{d}^{ds} = Rs^{ds}$, and

$$\frac{1}{R} \equiv \frac{\langle x \rangle_{s+\bar{s}}}{\langle x \rangle_{\bar{u}+\bar{d}}(DI)} = 0.822 \, \text{at} \, 1.3 \text{ GeV}$$

from lattice QCD, and considering the ansatzs of small-x behavior, we obtain the CT18CS at $Q_0 = 1.3$ GeV scale.

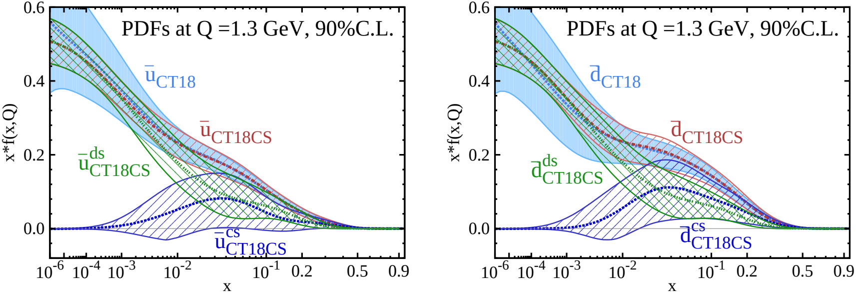

CT18CS PDFs

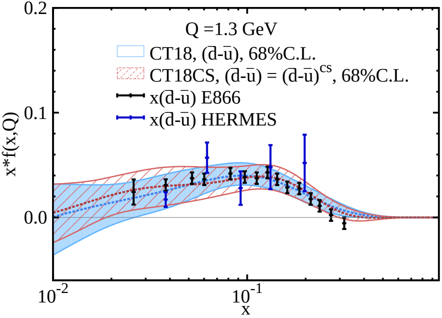

$$
\begin{aligned}
&\bar{d} - \bar{u} \\
&\quad = (\bar{d}^{cs} + \bar{d}^{ds}) - (\bar{u}^{cs} + \bar{u}^{ds}) \\
&\quad = \bar{d}^{cs} - \bar{u}^{cs}
\end{aligned}
$$

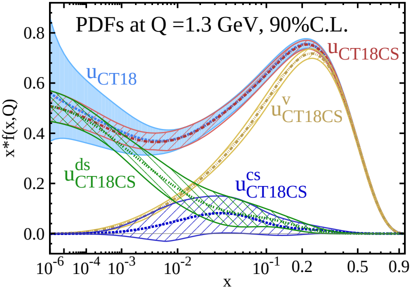

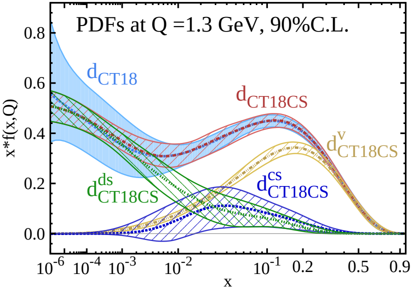

CT18CS PDFs

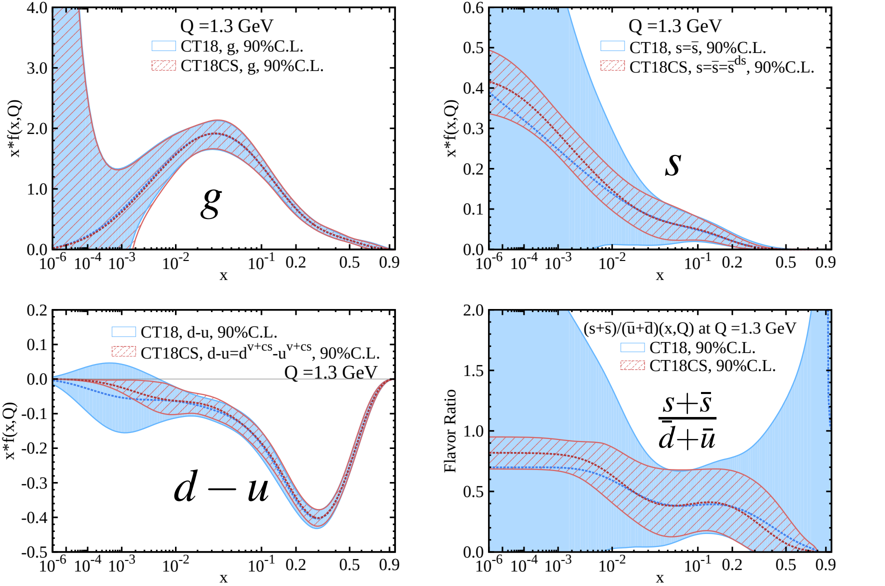
Q =1.3 GeV
CT18, g, 90%C.L.
CT18CS, g, 90%C.L.
g
x*f(x,Q)
x
Q =1.3 GeV
CT18, s=s̄, 90%C.L.
CT18CS, s=s̄=s̄ds, 90%C.L.
s
x*f(x,Q)
x
CT18, d-u, 90%C.L.
CT18CS, d-u=dv+cs-uv+cs, 90%C.L.
Q =1.3 GeV
d − u
x*f(x,Q)
x
(s+s̄)/(ū+d̄)(x,Q) at Q =1.3 GeV
CT18, 90%C.L.
CT18CS, 90%C.L.
(s+s̄)/(d̄+ū)
Flavor Ratio
x

E906/SeaQuest

$$\frac{\sigma(pd)}{2\sigma(pp)}$$

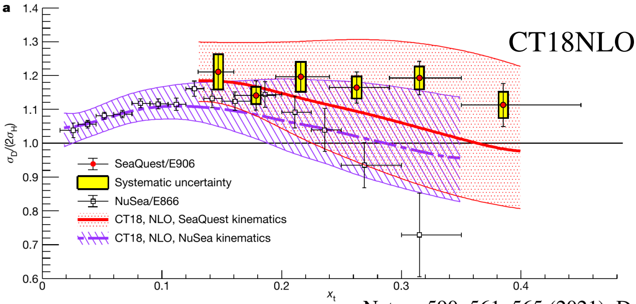

Nature 590, 561–565 (2021), Dove, J. *et al.*

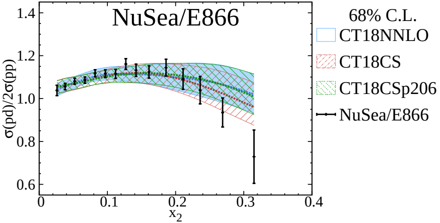

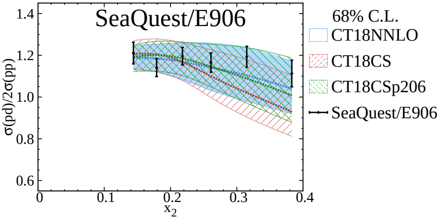

The $\langle x\rangle$ Moment of CT18CS at 1.3 GeV

The $\langle x\rangle$ moment of CT18 and CT18CS at 1.3 GeV:

PDF	$<x>_{u^v}$	$<x>_{d^v}$	$<x>_g$	$<x>_{\bar{u}}$	$<x>_{\bar{d}}$	$<x>_s$
CT18	0.325(5)	0.134(4)	0.385(10)	0.0284(22)	0.0361(27)	0.0134(52)
CT18CS	0.323(4)	0.136(3)	0.384(12)	0.0287(25)	0.0364(34)	0.0137(39)

PDF	$<x>_{u^{v+cs}}$	$<x>_{d^{v+cs}}$	$<x>^{\star}_{\bar{u}^{cs}}$	$<x>^{\star}_{\bar{d}^{cs}}$	$<x>^{\S}_{u^{ds}}$
CT18CS	0.335(7)	0.155(8)	0.0120(64)	0.0197(70)	0.0167(49)

More direct comparison between global analysis and lattice calculation can be done for each parton degree of freedom, instead of being limited to $u-d$ and s.

	$Q=2.0$ GeV		$Q=1.3$ GeV	
	CT18	Lattice	CT18CS	CT18
$\langle x\rangle_{u^+-d^+}$	0.156(7)	$0.111-0.209^{N_f=2+1}$ $0.153-0.194^{N_f=2+1+1\dagger}$ $0.166-0.212^{N_f=2}$	0.173(7)	0.175(8)
$\langle x\rangle_{s^+}$	0.033(9)	$0.051(26)(5)^{\ddagger}$	0.027(8)	0.027(10)

† Prog. Part. Nucl. Phys., 121:103908, 2021. ‡ Phys. Rev. Lett., 121(21):212001, 2018

$$u^+-d^+=(u+\bar{u})-(d+\bar{d})=(u^{v+cs}+u^{ds}+\bar{u}^{cs}+\bar{u}^{ds})-(d^{v+cs}+d^{ds}+\bar{d}^{cs}+\bar{d}^{ds})$$

$$\xrightarrow{CT18CS}(u^{v+cs}-d^{v+cs})+(\bar{u}^{cs}-\bar{d}^{cs})$$

$$s^+=s+\bar{s}=s^{ds}+\bar{s}^{ds}\xrightarrow{CT18CS}2s^{ds}$$

Impact of lattice Strangeness Asymmetry data in the CTEQ-TEA global analysis

In Collaborate with Huey-Wen Lin, Mengshi Yan, C.-P. Yuan
arXiv:2211.11064

CT18 with $s(x) \neq \bar{s}(x)$

In the framework of CT18, 6 d.o.f of partons are parametrized at $Q_0 = m_c = 1.3$ GeV.

$$g, \quad u^v, \quad d^v, \quad \bar{u}, \quad \bar{d}, \quad s.$$

Where $\bar{s}(x) \equiv s(x)$ is assumed. The number sum rule for strangeness is satisfied naively. Because the DGLAP equation preserve

$$\int_0^1 [s(x) - \bar{s}(x)]dx = 0,$$

People used to parametrize the strange as $s_+ = s + \bar{s}$ and $s_- = s - \bar{s}$. For example, in CTEQ 6

$$s_+(x, Q_0) = a_0^s x^{a_1 - 1}(1-x)^{a_2} P_+(x)$$
$$s_-(x, Q_0) = s_+(x, Q_0)\tanh[ax^b(1-x)^c P_-(x)]$$

$$P_-(x) = \left(1 - \frac{x}{x_0}\right)(1 + dx + ex^2 + ...)$$

CT18 with $s(x) \neq \bar{s}(x)$

We consider an alternative way on parametrizing the strangeness. Consider both s and $\bar{s}$ contain an overall factor a_0 :

$$s(x, Q = Q_0) = a_0^s x^{a_1^s - 1}(1-x)^{a_2^s} P^s(x) = a_0^s g^s(x)$$

$$\int_0^1 [a_0^s g^s(x) - a_0^{\bar{s}} g^{\bar{s}}(x)] dx = 0$$

By given $a_0^{\bar{s}}$, the a_0^s can be determined by the strange number sum rule.

$$a_0^s = \frac{\int a_0^{\bar{s}} g^{\bar{s}}(x) dx}{\int g^s(x) dx}$$

- Different from the root-finding method, there is no presumed requirement on the function form of $g^s(x)$ and $g^{\bar{s}}(x)$.
- But it is relatively hard to control the number of crossing in $s - \bar{s}$.

CT18As NNLO: CT18A with Strangeness Asymmetry

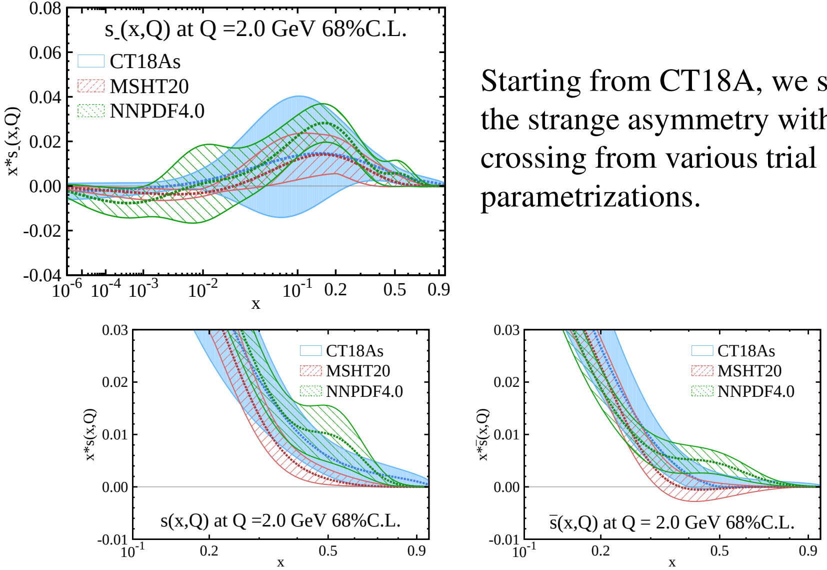

Starting from CT18A, we select the strange asymmetry with single crossing from various trial parametrizations.

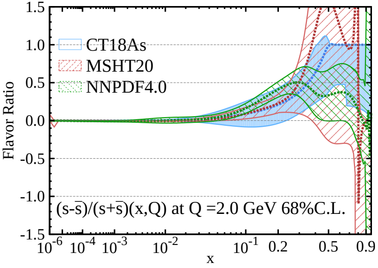

Asymmetry norminally reaches $\sim 50\%$ at $x \sim 0.25$ in three global fits.

$s_- \neq 0$ is preferred by LHC Drell-Yan processes and E866 p/d ratio.

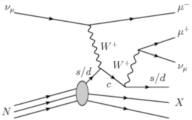

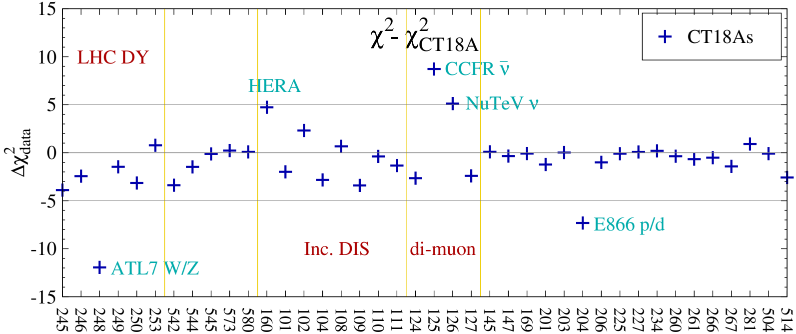

First Lattice Strange PDF

§ On the lattice, one needs to calculate the following

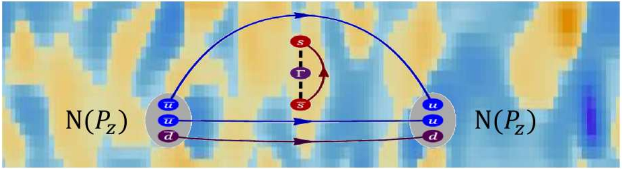

2005.12015, Zhang, Lin, Yoon

§ Results by MSULat/quasi-PDF method

- Clover on 2+1+1 HISQ 0.12-fm 310-MeV QCD vacuum
  - 7,184,000 strange loops
  - 344,832 nucleon correlators
- RI/MOM renormalization
- Extrapolated to
  $M_\pi \approx 140$ MeV

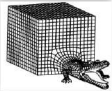

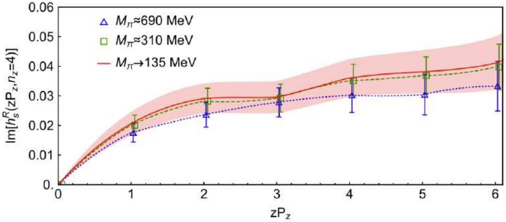

First Lattice Strange PDF

§ Lattice matrix elements

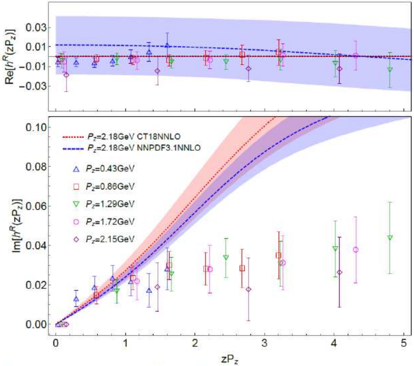

➢ Strange-antistrange symmetry

$$\mathrm{Re}[h(z)] \propto \int dx\,(s(x) - \bar{s}(x))\cos(xzP_z)$$

$$\mathrm{Im}[h(z)] \propto \int dx\,(s(x) + \bar{s}(x))\sin(xzP_z)$$

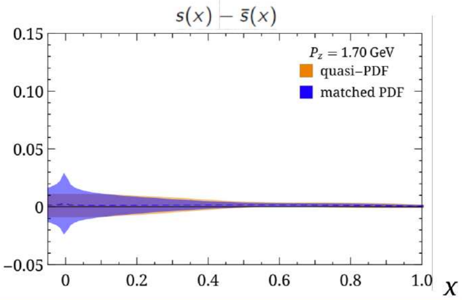

§ From quasi-PDF to PDF

$$\tilde{f}_q(x, P_z) = \int_{-1}^{1} \frac{dy}{|y|} f_q(y) C_{q/q}(x, y, P_z, \mu)$$

$$+O\left(\frac{\Lambda_{QCD}^2}{x^2 P_z^2}, \frac{\Lambda_{QCD}^2}{(1-x)^2 P_z^2}\right)$$

CT18As_Lat: Strangeness asymmetry with a lattice QCD constraint

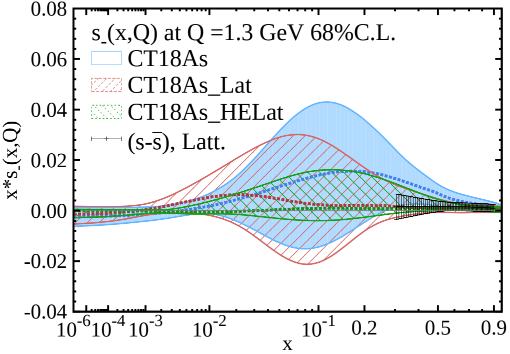

CT18As:
CT18A with strange asymmetry.
CT18As_Lat:
PDFs with lattice input.
CT18As_HELat:
PDFs if the lattice errors are reduced by 1/2.

- Lattice QCD calculation provide prediction for $0.3 < x < 0.8$.
- Lattice QCD prediction disfavors a large $s_{-}(x, Q)$ for $x > 0.3$ region. It cause the reduction in $s_{-}(x, Q)/s_{+}(x, Q)$ for $x < 0.3$ (depending on the parametrization form).

CT18As_Lat:
Strangeness asymmetry with a lattice QCD constraint

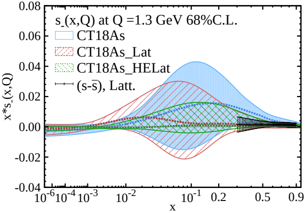

Di-muon data provide measurments for $0.015 < x < 0.336$.

DIS and dimuon SIDIS show less clear trends.

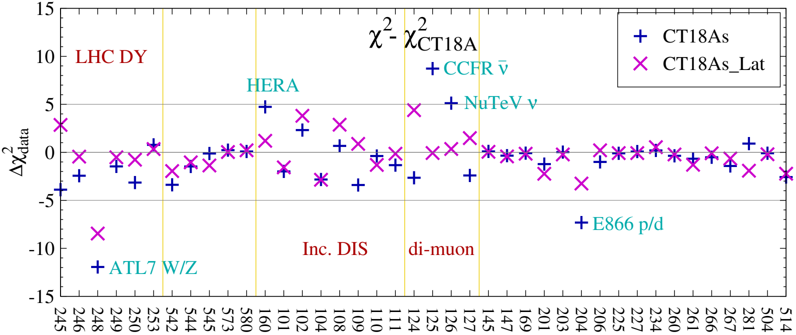

Summary

- PQCD and LQCD are both important methods for studying the structure of hadron. But there were only few physical quantities can be used for comparison is the past.

- With the input from lattice QCD, $\frac{1}{R} \equiv \frac{\langle x \rangle_{s+\bar{s}}}{\langle x \rangle_{\bar{u}+\bar{d}}(DI)}$, we consider global analysis with the connected sea parton degrees of freedom taken into account, which are respondsible for $\bar{u} \neq \bar{d}$, as suggested by data. The result of global analysis, the CT18CS, is found to be compatible with CT18.

- The CT18CS allows to provide direct comparison between lattice calculations and global analysis for each parton degree of freedom.

Summary

- Lattice QCD calculation disfavors a large $s_-(x, Q)$ for $x > 0.3$.
- By treating lattice QCD calculation as data, we have chance to determine PDFs at $x \to 1$.
- The framework of global analysis provide indirect comparsion between lattice calculations and experimental measurements in the overlap region.

Hadronic tensor in Euclidean path-integral formalism

- DIS in Minkowski space $\frac{d^2\sigma}{dE'd\omega} = \frac{\alpha^2}{q^4}\frac{E'}{E} l^{\mu\nu} W_{\mu\nu}$

$$W_{\mu\nu}(\vec{q},\vec{p},\nu) = \frac{1}{\pi}\mathrm{Im}T_{\mu\nu} = \langle N(\vec{p})|\int \frac{d^4x}{4\pi} e^{iq\cdot x} J_\mu(x) J_\nu(0)|N(\vec{p})\rangle_{spin\ ave.}$$
$$= \frac{1}{2}\sum_n \int \prod_{i=1}^{n}\left[\frac{d^3p_i}{(2\pi)^3 2E_{pi}}\right](2\pi)^3\delta^4(p_n - p - q)\langle N(\vec{p})|J_\mu(0)|n\rangle\langle n|J_\nu(0)|N(\vec{p})\rangle_{spin\ ave.}$$

- Euclidean path-integral

(K.F. Liu and S.J. Dong, PRL 72, 1790 (1994), K.F. Liu, PRD 62, 074501 (2000))

$$\widetilde{W}_{\mu\nu}(\vec{q},\vec{p},\tau)$$
$$= \frac{1}{4\pi}\sum_n \frac{2m_N}{E_n}\delta(\vec{p}_n - \vec{p} - \vec{q}) < N(\vec{p})|J_\mu|n >< n|J_\nu|N(\vec{p}) >_{spin\ ave.}\ e^{-(E_n - E_p)\tau}$$
$$= < N(\vec{p})|\sum_{\vec{x}} \frac{e^{-i\vec{q}\cdot\vec{x}}}{4\pi} J_\mu(\vec{x},\tau) J_\nu(0,0)|N(\vec{p}) >_{spin\ ave.}$$

Inverse problem (Laplace transform)

$$D(\tau) = \int K(\tau,\nu)\rho(\nu)d\nu,$$
$$D(\tau) = \widetilde{W}_{\mu\nu}(\tau), \quad K(\tau,\nu) = e^{-\nu\tau}, \quad \rho(\nu) = W_{\mu\nu}(q^2,\nu)$$